

OMAE2008-57525

EXPERIMENTAL RESULTS OF TSUNAMI BORE FORCES ON STRUCTURES

I.N. Robertson

Dept of Civil and Environmental Engineering
University of Hawaii at Manoa
Honolulu, Hawaii 96822

H. R. Riggs

Dept of Civil and Environmental Engineering
University of Hawaii at Manoa
Honolulu, Hawaii 96822

A. Mohamed

Dept of Ocean and Resources Engineering
University of Hawaii at Manoa
Honolulu, Hawaii 96822

ABSTRACT

A series of experiments has been carried out at the Tsunami Wave Basin (TWB) at Oregon State University (OSU) to determine the effect of tsunami bores on coastal and near-shore structures, especially buildings and bridges. The TWB is equipped with a piston-type wavemaker capable of generating clean solitary waves. The facility was used to model tsunami bores breaking over coastal reefs and their impact on structural components, including columns, walls, and horizontal members, such as building floors and bridge decks. Detailed wave height and velocity measurements were recorded as well.

This paper focuses on the fluid forces of a bore impacting a wall/floor system. The experimental setup will be described and force results will be presented. The experimental results provide needed data to validate CFD models that can then be used to determine forces for a wider variety of situations.

INTRODUCTION

Coastal buildings, bridges, highways, and harbor facilities that are at risk of tsunami inundation may suffer significant damage if the structures are not adequately designed for the fluid loading. Ref. [1-3] document damage from scour and fluid loading from the 2004 Great Indian Ocean Tsunami. The structural damage is strikingly similar to what can happen from hurricane storm surge and waves [4, 5]. Damage of floors from vertical fluid forces as a result of Hurricane Katrina is shown in Figure 1 and 2. Although there are some clear differences between the damage mechanisms of tsunami and hurricane surge/waves, there are also clear similarities in the damage.

The quantification of wave impact forces on structures has received significant attention over the years. The work can be categorized into three areas. Probably one of the most studied

is the issue of storm wave impact on offshore platforms. A sampling of work, spanning experimental and numerical attempts to develop design formulas for the loads, can be found in [6-18]. The second area is storm wave breaking on coastal structures, especially seawalls and breakwaters [19-26]. Much less studied are the forces resulting from tsunami bores/surges hitting coastal structures [27-30].

Tsunami engineering, the focus of a 2007 special issue of the ASCE *Journal of Waterway, Port, Coastal and Ocean Engineering*, was defined therein as ‘those activities that are significant for the engineering goal of designing and protecting the built environment and the people that dwell therein, with regard to potential tsunami hazards’ [31]. While this has received more attention recently, designers of onshore facilities typically have very little experience and receive very little guidance in tsunami induced loads that should be considered for bridge and building design [32, 33]. In addition, the simulation of these loads is very complex and it pushes the state-of-the-art in computational fluid dynamics (CFD).

The US National Science Foundation (NSF) has initiated a program to improve the understanding of tsunamis and their threat to the built environment. One aspect of this initiative is the funding of the NSF Network for Earthquake Engineering Simulation (NEES), which includes Oregon State University’s (OSU) Tsunami Wave Basin, shown in Figure 3. The rectangular basin is 48.8 m x 26.5 m x 2.1 m. The maximum water depth is 1.3 m, resulting in a freeboard of 0.8 m. The wavemaker is an electric motor driven piston-type, consisting of 29 boards, each 2.0 m high. Regular, irregular, and solitary (tsunami) waves can be generated, both single and multi-directional. The wave periods range from 0.5 s to 10 s. The pistons have a maximum stroke of 2.1 m and a maximum

velocity of 2.0 m/s. More information on the facility can be found on the web [34].

The authors are investigators on an NSF-funded project utilizing the TWB. The project is titled ‘Development of Performance-Based Tsunami Engineering, PBTE’, and its goal is to develop the methodology and validated simulation tools for implementation of site specific PBTE for use in the analysis, evaluation, design and retrofit of coastal structures and facilities, as well as the development of code-compatible provisions for tsunami-resistant structural design.

The project’s experimental component focuses on tsunami 1) run-up and inundation, including fluid velocities and energy dissipation; 2) fluid loading on structural elements; and 3) sediment transport and scour as a result of inundation and drawdown.



Figure 1. Double-tee negative bending failure in parking structure at Grand Casino, Biloxi – bottom picture is inset from top picture [5]



Figure 2. Parking garage post-tensioned flat slab destroyed by hydrodynamic uplift forces. Note concrete shear wall and ramp obstructing flow through the building [5]

The primary objective of the experimental component of the project is to provide data to validate numerical models for each of these 3 areas. A recent publication [35] described the different experimental setups in some detail. This paper focuses on the fluid forces of a bore impacting a wall/floor system. The experimental setup will be described and force results will be presented. The experimental results are useful to validate simulation of bore impact with CFD models.

EXPERIMENTAL SETUP

We used a number of beach slopes and fringing reef configurations, but unfortunately the TWB does not have a reconfigurable beach. Because of this, and because we were mostly interested in two-dimensional flow, we constructed two, 2.16 m wide flumes in the TWB, as shown in Figure 4.



Figure 3. Tsunami Wave Basin (TWB) [34]



Figure 4. Flumes in the TWB

The experiments described herein involved a 1:15 beach slope and a ‘fringing reef’, i.e., a flat section over which the bore/surge propagates. The beach slope terminated 1 m above the basin bottom, as shown in Figure 5. The beach and reef were smooth concrete. Water depths of 1.0 and 1.10 m and solitary wave heights of 0.2, 0.4, and 0.6 m were used.

The incoming solitary wave transforms to a turbulent bore/surge at the transition between the beach slope and the fringing reef. This bore/surge then impinges the structural test specimen located at 35 meters from the wave maker as shown in Figure 5. Immediately prior to impact, the surface shape and velocity were recorded by a laser surface profiler, LSP, by filming the water surface reflection of a vertical laser sheet oriented along the centerline of the wave channel. Post-processing of the video capture of this laser image was used to determine bore height, velocity and leading edge shape.

Figure 6 shows the wall and floor slab system installed in the wave flume. The wall behind the floor slab is rigidly attached to the concrete flume base. The floor slab was divided into 3 sections. The two outer aluminum sections are rigidly supported from a structural frame above the flume and the flume side walls. The middle acrylic floor section is supported independently of the other floor and wall elements and instrumented to measure vertical load. The two load cells supporting the test floor slab were monitored at 1000 Hz throughout each wave impact (Figure 7). Figure 8 shows the impact of a bore traveling from behind the camera location and reflecting off the floor slab and wall test configuration.

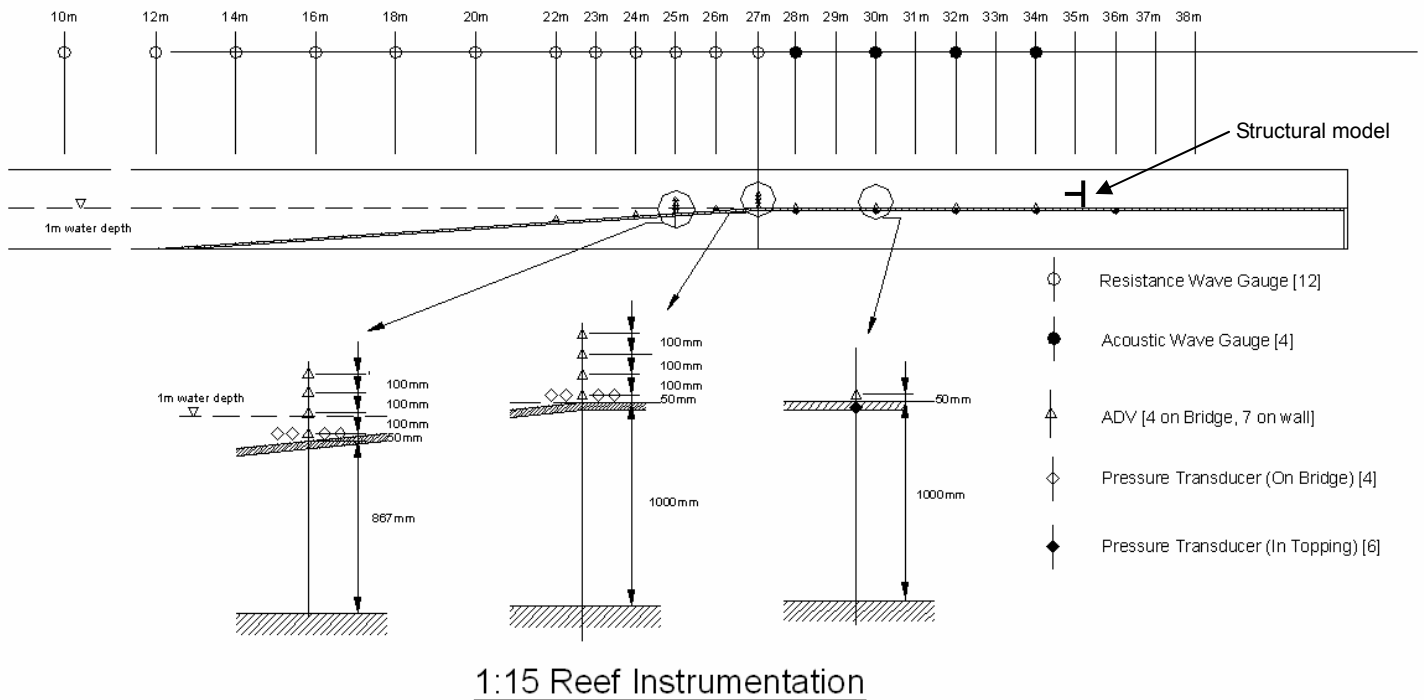


Figure 5 Beach slope and fringing reef with instrumentation



Figure 6: Wall and floor slab test setup

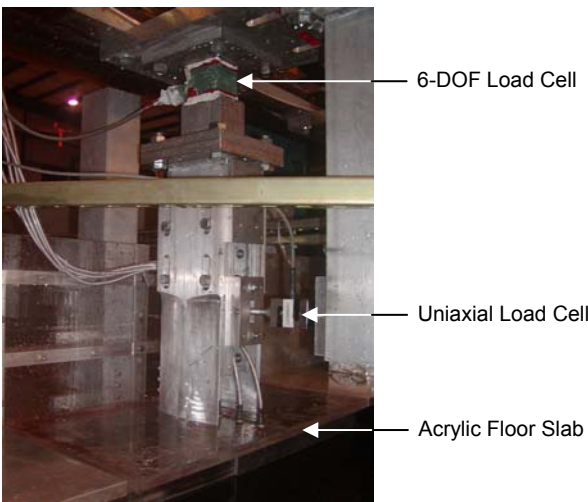


Figure 7: Details of floor slab instrumentation



Figure 8: Bore impact on wall and floor test configuration

EXPERIMENTAL RESULTS

The water level in the wave basin was varied from 1.00 m to 1.10 m so as to change the still water level on the flat reef. For a water level of 1.00 m, there was no water on the flat reef. For water levels of 1.10 m the still water on the flat reef was 10 cm deep. The model floor slab was maintained at 10 cm above the still water level. Solitary waves with heights of 20, 40 and 60 cm were propagated over the 1:15 beach upstream of the structural model. Wave breaking occurred at the edge of the reef resulting in a turbulent bore advancing over the flat reef towards the structural model. The characteristics of this bore were captured using a Laser Surface Profiler (LSP) located immediately in front of the structural model. Each wave configuration was repeated a minimum of three times. Table 1 lists the average bore height and velocity for each size solitary wave and each level of still water on the reef.

Table 1: Laboratory bore characteristics

Still water depth on reef (cm)	Solitary Wave Height (cm)	Bore height H_b (cm)	Bore velocity V_b (cm/s)	Froude Number
0	20	6.0	191	2.49
	40	13.1	310	2.73
	60	16.6	375	2.94
10	20	8.1	193	2.17
	40	14.8	220	1.82
	60	19.9	299	2.14

Figure 9 and Figure 10 show the relationship between bore height and velocity with the initial solitary wave height for both the 1.00m and 1.10 m water levels. The error bars show maximum and minimum recorded values. As expected, a larger solitary wave produces a larger bore with higher velocity. Bores traveling over a dry bed have smaller depth, but greater velocity. The presence of standing water on the reef has the effect of slowing the bore, except in the case of the smallest wave height, and causing the bore depth to increase.

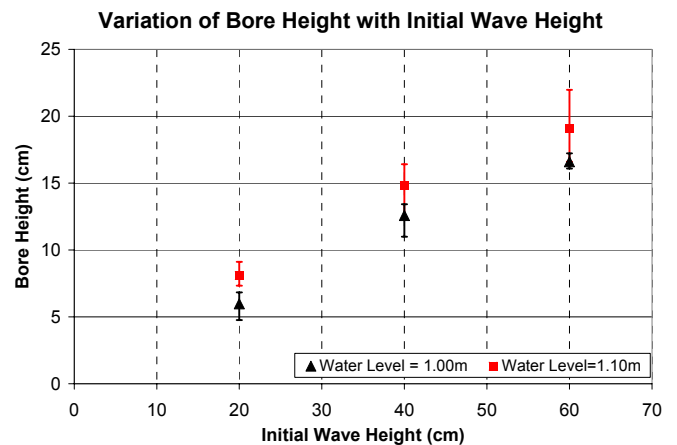


Figure 9: Variation of bore height with initial wave height

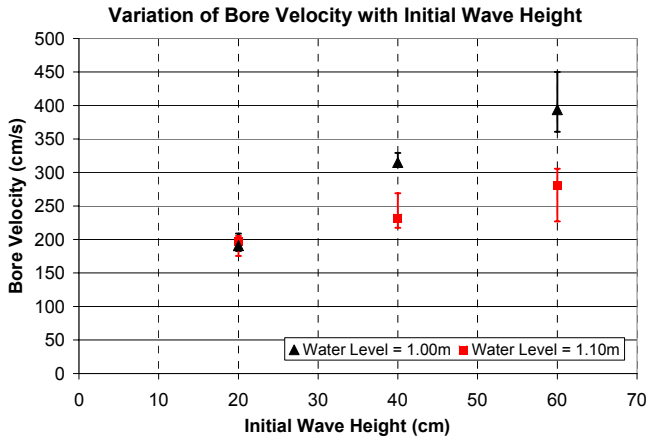
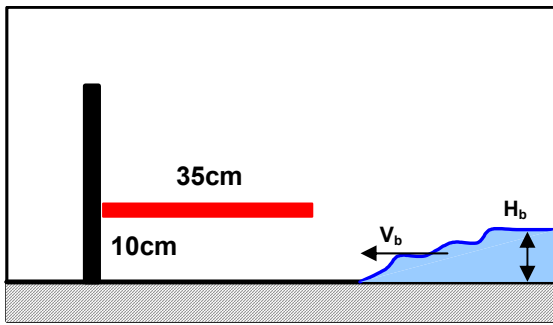


Figure 10: Variation of bore velocity with wave height

Figure 11 and Figure 12 show time histories of the average pressure induced on the soffit of the floor slab for a number of bores produced by equal size solitary waves. The time scale starts with initiation of the wavemaker. Note that the vertical scales differ so as to increase plot clarity. The variation in time

history between nominally identical incoming waves appears to be related to the turbulent nature of the leading edge of the bore as it propagates over the flat reef. These variations are greater for the case with 10 cm standing water on the reef indicating that this condition leads to greater turbulence in the bore leading edge than the dry reef condition. Each time history is characterized by a steep loading ramp to a peak impulsive load followed by a rapid decrease to a sustained, though fluctuating, residual uplift. This residual uplift dissipates with time as the water drains off the reef area.

For the dry reef condition, the initial impulsive load has a duration on the order of 0.05 to 0.1 second, while the residual uplift varies from 15 to 30 percent of the peak uplift pressure (Figure 11). For the reef with 10 cm standing water, the initial impulsive load has a duration on the order of 0.06 to 0.15 second, while the residual uplift varies significantly for different wave heights, and even within the same wave height regime (Figure 12). This variability is attributed to greater turbulence in the bores traveling over standing water on the reef flat.



Wall-slab test configuration with incoming bore

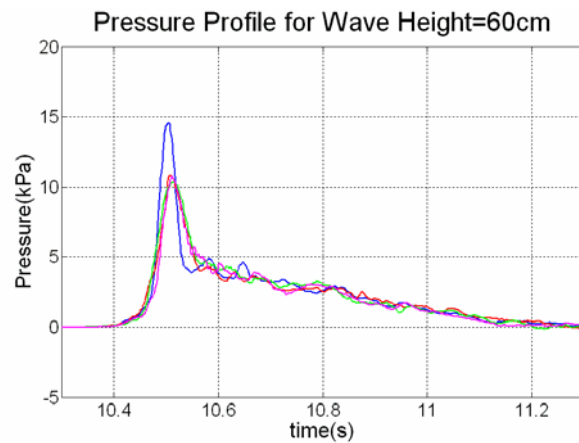
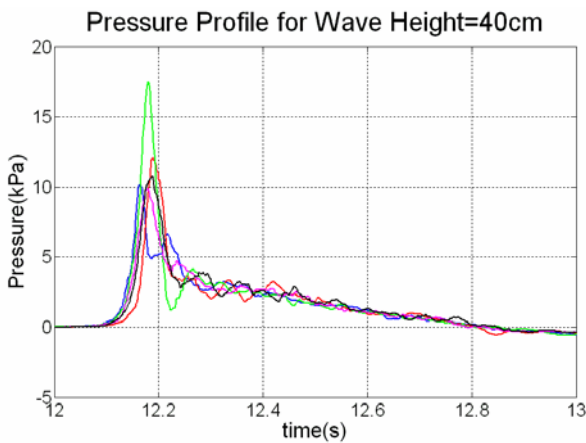
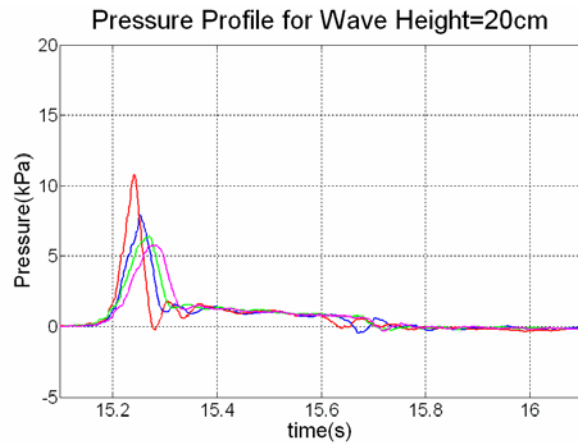
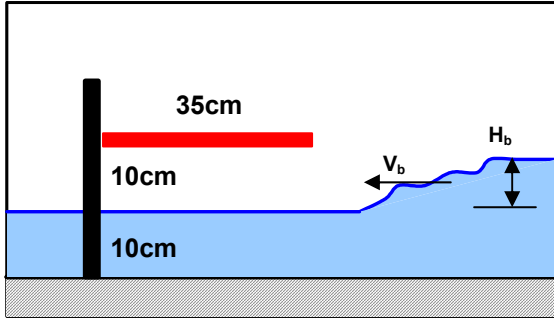


Figure 11: Uplift pressure on floor slab for bores caused by 20, 40 and 60 cm solitary waves with no water on reef



Wall-slab test configuration with incoming bore

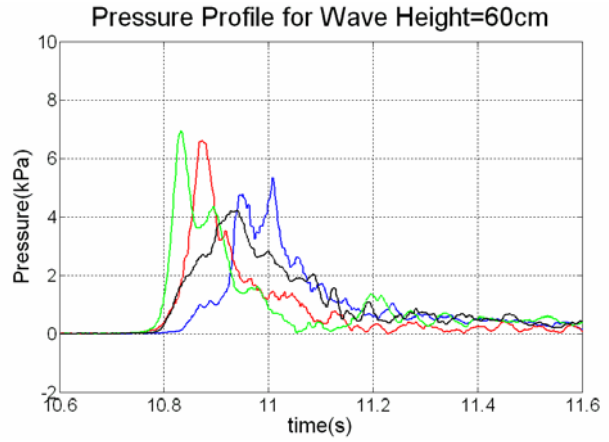
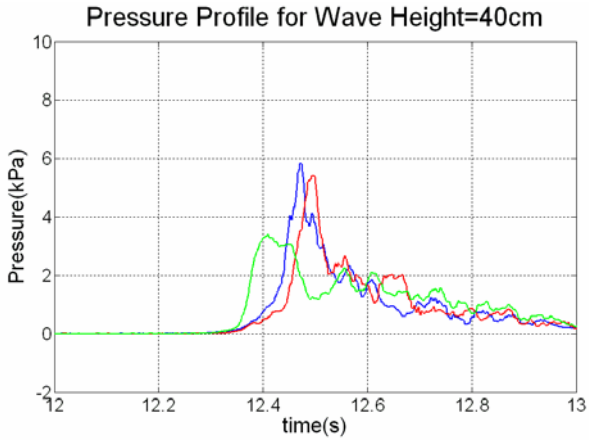
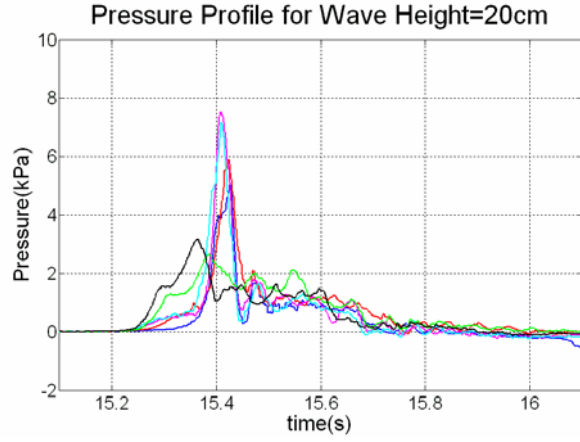


Figure 12: Uplift pressure on floor slab for bores caused by 20, 40 and 60 cm solitary waves with 10 cm water on reef

For the dry reef condition, the maximum uplift pressures are produced by the 40 and 60 cm solitary waves, each of which had bore heights exceeding the 10 cm height of the slab soffit. Peak uplift pressures for this condition range from 10 to 17 kPa (Figure 11 and Figure 13). Uplift pressures for the 20 cm solitary waves with bore height of 6.0 cm were lower, ranging from 6 to 11 kPa. The shape of the impulsive load time history appears more consistent for the larger wave sizes (Figure 11).

For the reef with 10 cm standing water, and the slab soffit at 10 cm above this water level, there is considerable variability in the peak uplift pressures for nominally identical waves with a range from 3 to 7.5 kPa (Figure 12). However, the average peak uplift pressure is fairly consistent even though the bore height varies from 8.1 to 19.9 cm (Figure 13). As with the dry reef case, it appears that the maximum uplift is achieved when the bore depth is at or close to the clear height below the slab, and does not increase when the bore depth is greater than this height.

MODEL TO PROTOTYPE SCALING

Scaling of experimental results to prototype conditions is challenging. Froude scaling is commonly used for free surface gravity flows. The Froude number is given by v/\sqrt{gd} , where v is the bore velocity, d is the bore height, and g is the acceleration due to gravity. If the length ratio between prototype (L_p) and model (L_m) is $L = L_p/L_m$ then the bore properties would scale as follows:

$$\text{Velocity: } v_p = v_m \sqrt{L} \quad \text{Eqn. 1}$$

$$\text{Time: } t_p = t_m \sqrt{L} \quad \text{Eqn. 2}$$

$$\text{Pressure: } p_p = p_m L \quad \text{Eqn. 3}$$

Scaling an experimental bore height of 13.1 cm (resulting from a 40 cm solitary wave on dry reef) to a tsunami bore height of 2 m requires a scaling factor $L \approx 15$. Applying this Froude scaling to the bore characteristics in Table 1 results in the prototype bore characteristics shown in Table 2. As expected the Froude numbers are consistent.

Table 2: Prototype bore characteristics

Still Water level on reef (m)	Solitary Wave Height (m)	Bore height H_b (m)	Bore velocity V_b (m/s)	Froude Number
0	3	0.90	7.4	2.49
	6	1.97	12.0	2.73
	9	2.49	14.5	2.94
1.50	3	1.22	7.5	2.17
	6	2.22	8.5	1.82
	9	2.99	11.6	2.14

Figure 13 shows the average peak uplift pressure, along with maximum and minimum values, for the model slab. Scaling these pressures to prototype conditions using Froude scaling would result in the uplift pressures shown in Figure 14. These pressures are significantly larger than dead weight of a typical floor system. For example, a 20 cm thick concrete flat slab has a dead weight of only 4.8 kPa. Typical floor live loads used in design range from 2.5 to 12 kPa depending on the building occupancy. Clearly the impulsive upward loads caused by a tsunami bore passing under a floor slab with a solid wall obstructing through flow would result in uplift failure of the floor system. This could explain some of the floor and deck slab failures observed after the Indian Ocean tsunami of 2004 [36].

It is of course unclear that the model results can be scaled to prototype with simple Froude scaling. To investigate this, further experiments are planned in the Large Wave Flume at OSU where a new tsunami wave maker is being installed. These tests will be 2.5 times larger than those reported here. Numerical simulations using computational fluid dynamics (CFD) are also underway to verify the model to prototype scaling.

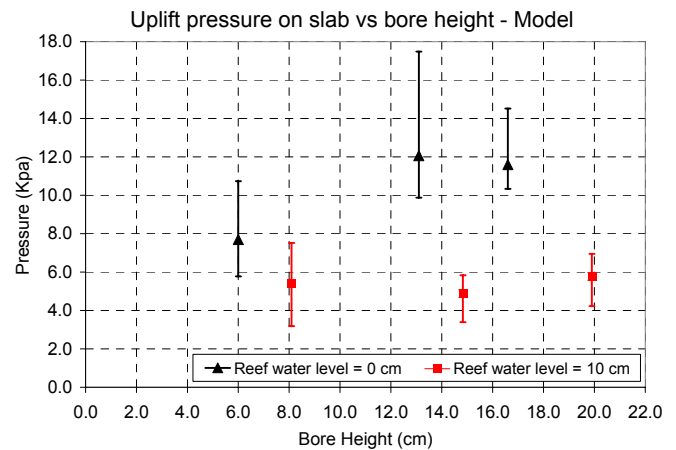


Figure 13: Model uplift pressure vs. bore height

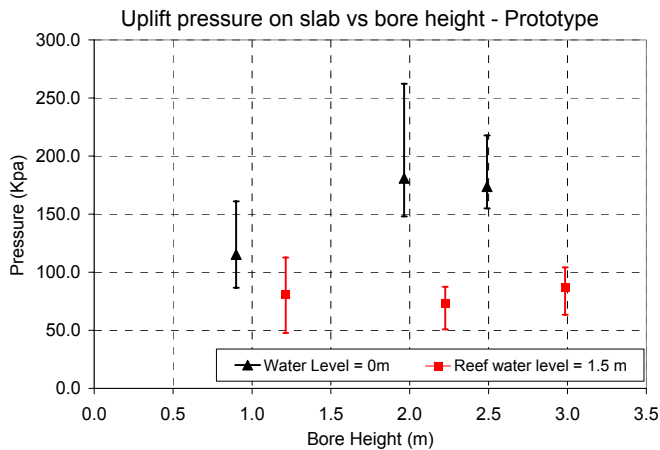


Figure 14: Prototype uplift pressure vs. bore height

CONCLUSIONS

This paper presents preliminary results of a study to quantify the uplift loads on a structural floor slab when subjected to different size tsunami bores. A solid wall at the back of the structural model prevents the bore from passing through the model. Based on these experiments, the following conclusions were drawn:

- Impulsive uplift loads induced on floor slabs when a tsunami bore is prevented from flowing through the building can be significantly larger than the uplift capacity of typical concrete floor construction.
- The maximum impulsive uplift loads occur when the bore depth is equal to the story height. Bore depths that exceed the story height produce uplift loads equal to this maximum condition. Bore depths smaller than the story height produce lower uplift loads.
- There is significant variability in the impulsive uplift pressures induced on the slab soffit. This is attributed to the turbulent nature of the incoming bore, and is more significant for the condition where the bore travels over standing water in its approach to the model.

ACKNOWLEDGMENTS

Funding for this research was provided by the National Science Foundation through the NSF George E. Brown, Jr. Network for Earthquake Engineering Simulation (grant #0530759). This funding is gratefully acknowledged. In addition, the authors would like to acknowledge the important contributions to the experiments of Geno Pawlak, graduate student Volker Roeber, and the OSU staff of the TWB.

REFERENCES

- [1] Saatcioglu, M., Ghobarah, A., Nistor, I., 2005, 'Reconnaissance Report on The December 26, 2004 Sumatra Earthquake and Tsunami,' Report The Canadian Association for Earthquake Engineering, 21 pp.
- [2] Yeh, H., Francis, M., Peterson, C., Katada, T., Latha, G., Chadha, R.K., Singh, J.P., Rahghuraman, G., 2007, 'Effects of the 2004 Great Sumatra Tsunami: Southeast Indian Coast,' Journal of Waterway, Port, Coastal, and Ocean Engineering, 133, pp. 382-400.
- [3] Sundar, V., Sannasiraj, S.A., Murali, K., Sundaravadivelu, R., 2007, 'Runup and inundation along the Indian peninsula, including the Andaman Islands, due to Great Indian Ocean Tsunami,' Journal of Waterway, Port, Coastal, and Ocean Engineering, 133, pp. 401-413.
- [4] Robertson, I., Riggs, H.R., Yim, S., Young, Y.L., 2006, 'Lessons from Katrina,' ASCE Civil Engineering magazine, April, pp. 56-63.
- [5] Robertson, I.N., Riggs, H.R., Yim, S.C.S., Young, Y.L., 2007, 'Lessons from Hurricane Katrina storm surge on bridges and buildings,' Journal of Waterway, Port, Coastal, and Ocean Engineering, 133, pp. 463-483.
- [6] Baarholm, R., Faltinsen, O.M., 2004, 'Wave impact underneath horizontal decks,' Journal of Marine Science and Technology, 9, pp. 1-13.
- [7] Bea, R.G., Iverson, R., Xu, T., 2001, 'Wave-in-deck forces on offshore platforms,' Journal of Offshore Mechanics and Arctic Engineering, 123, pp. 10-21.
- [8] Bea, R.G., Xu, T., Stear, J., Ramos, R., 1999, 'Wave forces on decks of offshore platforms,' Journal of Waterway, Port, Coastal, and Ocean Engineering, 125, pp. 136-144.
- [9] Cuomo, G., Tirindelli, M., Allsop, W., 2007, 'Wave-in-deck loads on exposed jetties,' Coastal Engineering, 54, pp. 657-679.
- [10] Iwanowski, B., Grigorian, H., Scherf, I., 2002, 'Subsidence of the Ekofisk platforms: Wave in deck impact study. Various wavemodels and computational methods,' Proc., 21st International Conference on Offshore Mechanics and Arctic Engineering, paper OMAE2002-28063, 8 pp.
- [11] Kaplan, P., 1979, 'Impact forces on horizontal members,' Proc., Civil Engineering in the Oceans, pp. 716-731.
- [12] Kaplan, P., 1992, 'Wave impact forces on offshore structures: re-examination and new interpretations,' Proc., Offshore Technology Conference, pp. 79-86.
- [13] Kaplan, P., Murray, J.J., Yu, W.C., 1995, 'Theoretical analysis of wave impact forces on platform deck structures,' Proc., Offshore Mechanics and Arctic Engineering, pp. 189-198.
- [14] Ren, B., Wang, Y., 2003, 'Experimental study of irregular wave impact on structures in the splash zone,' Ocean Engineering, 30, pp. 2363-2377.
- [15] Ren, B., Wang, Y., 2004, 'Numerical simulation of random wave slamming on structures in the splash zone,' Ocean Engineering, 31, pp. 547-560.

- [16] Shih, R.W.K., Anastasiou, K., 1992, 'A laboratory study of the wave-induced vertical loading on platform decks,' Proceedings, Institution of Civil Engineers-Water, Maritime & Energy, 96, pp. 19-33.
- [17] van Raaij, K., Gudmestad, O.T., 2007, 'Wave-in-deck loading on fixed steel jacket decks,' Marine Structures, 20, pp. 164-184.
- [18] Wang, H., 1970, 'Water wave pressure on horizontal plate,' Journal of the Hydraulics Division, ASCE, 96, pp. 1997-2016.
- [19] Chan, E.-S., Melville, W.K., 1989, 'Plunging wave forces on surface-piercing structures,' Journal of Offshore Mechanics and Arctic Engineering, 111, pp. 92-100.
- [20] Chan, E.S., Melville, W.K., 1988, 'Deep-water plunging wave pressures on a vertical plane wall,' Proc. Royal Society of London. Series A, Mathematical and Physical Sciences, 417, pp. 95-131.
- [21] Bullock, G., Obhrai, C., Müller, G., Wolters, G., Peregrine, H., Bredmose, H., 2003, 'Field and laboratory measurement of wave impacts,' Proc., Coastal Structures 2003, pp. 343-355.
- [22] Bullock, G.N., Obhrai, C., Peregrine, D.H., Bredmose, H., 2007, 'Violent breaking wave impacts. Part 1: Results from large-scale regular wave tests on vertical and sloping walls,' Coastal Engineering, 54, pp. 602-617.
- [23] Cooker, W.J., Peregrine, D.H., 1990, 'Violent water motion at breaking-wave impact,' Proc., 22nd Coastal Engineering Conference, pp. 164-176.
- [24] Wood, D.J., Peregrine, D.H., 1998, 'Two and three-dimensional pressure-impulse models of wave impact on structures,' Proc., Coastal Engineering Conference, pp. 1502-1515.
- [25] Peregrine, D.H., 2003, 'Water-wave impact on walls,' Annual Review of Fluid Mechanics, 35, pp. 23-43.
- [26] Cumberbatch, E., 1960, 'The impact of a water wedge on a wall,' Journal of Fluid Mechanics, 7, pp. 353-373.
- [27] Cross, R.H., 1967, 'Tsunami surge forces,' Journal of Waterways and Harbors Division, ASCE, 93, pp. 201-230.
- [28] Arnason, H., 2005, 'Interactions between an incident bore and a free-standing coastal structure,' PhD dissertation, University of Washington.
- [29] Yeh, H., 2007, 'Design tsunami forces for onshore structures,' Journal of Disaster Research, 2, pp. 1-6.
- [30] Arsen'ev, S.A., Zhivogina, O.A., Seliverstov, S.V., Shelkovnikov, N.K., 1998, 'Force action of tsunamis on different structures,' Atomic Energy, 85, pp. 497-500.
- [31] Riggs, H.R., 2007, 'JWPCOE Special Issue: Tsunami Engineering (Introduction),' Journal of Waterway, Port, Coastal, and Ocean Engineering, 133, 381 pp.
- [32] Yeh, H., Robertson, I., Preuss, J., 2005, 'Development of design guidelines for structures that serve as tsunami vertical evacuation sites,' Report 2005-4, Washington State Department of Natural Resources, 34 pp.
- [33] Yeh, H., Robertson, I.N., 2005, 'Development of design guideline for tsunami shelters,' Proc., First International Conference on Urban Disaster Reduction (1ICDR), 6 pp.
- [34] OSU, 2007, O.H. Hinsdale Wave Research Laboratory, <<http://wave.oregonstate.edu>>.
- [35] Riggs, H.R., Robertson, I.N., Cheung, K.F., Pawlak, G., Young, Y.L., Yim, S.C.S., 2008, 'Experimental simulation of tsunami hazards to buildings and bridges,' Proc., NSF CMMI Engineering Research and Innovation Conference, Paper No. 0530759, 8 pp.
- [36] Saatcioglu, M., Ghobarah, A., and Nistor, I. (2005). "Reconnaissance Report on the December 26, 2004 Sumatra Earthquake and Tsunami", Canadian Association for Earthquake Engineering, June 2005, 21 pp.